Thermodynamic and Kinetic Characterization of the Interaction between *N*-Butylamine and ∼1 nm CdSe Nanoparticles†

C. Landes and M. A. El-Sayed*

Laser Dynamics Laboratory, School of Chemistry and Biochemistry, Georgia Institute of Technology, Atlanta, Georgia 30332-0400

Received: January 16, 2002; In Final Form: April 30, 2002

When butylamine (0.1−0.25 M) is added to a colloidal solution of CdSe nanoparticles (NPs) that are 1−2 nm in diameter, the band gap absorption changes from a broad, relatively weak band centered at 445 nm to a narrow, relatively strong absorption centered at 414 nm. The effect of concentration on the observed spectrum shows an isobestic point, suggesting an equilibrium between two species. Thermodynamic and kinetic studies of this process were carried out. The transition was found to be exothermic, with a size-dependent heat of reaction that suggests that there is a direct proportionality between the NP size and the exothermicity of the interaction. The decay kinetics of the original peak were studied and compared to the rise kinetics of the 414 nm peak. The decay of the original NPs was biexponential, with a lifetime that depends on the NP size, concentration of reactants, and the temperature. The rise in the 414 nm peak was found to be multiexponential, reflecting transformations from the ensemble having different NP sizes. A mechanism is proposed for this interaction that depends on the binding of butylamine to the NP surface, followed by a release in energy. The nature of the new species absorbing at 414 nm is discussed.

Introduction

Semiconductor nanoparticles (NPs) are of interest because of their possible uses in catalysis,[1] energy storage,[2] and light source[3,4] applications. Because of quantum confinement and surface properties, the absorption and emission of these NPs can be size tuned.[5−8] Colloidal CdSe NPs within the size range from 2 to 10 nm prepared by the method reported by Murray et al.[9] are single crystals of the wurtzite form, prolate spheroid in shape, and characterized by regular crystal surfaces with widely interspersed defects that serve as carrier traps. Missing atoms, uncommon oxidation states, or adsorbed impurities are examples of the sort of defects that can act as carrier traps.[9−11] Whereas the size of the NP is apparent from the absorption properties,[9] the surface quality of the NP is related to the fluorescence.[6] Large NPs with regular surfaces are characterized by near band-edge or shallow-trap emission, and smaller NPs or those with a multitude of surface defects are dominated by deep-trap emission. Overcoating NPs with a wide band-gap semiconductor such as ZnS can eliminate the deep-trap emission that is associated with an irregular NP surface.[6]

When the NP size is reduced such that the particle is essentially all surface, the curvature of the surface is so high that virtually all of the surface atoms have a slightly different coordination and/or effective oxidation state. The experimental and theoretical studies of very small (1−2 nm) CdS[12,13] and CdSe[14,15] NPs are examples of such NP systems that are dominated by surface interactions.

Another factor that affects the stability of formation and storage of very small NPs is the contribution of geometrical stabilization. Large NPs are approximately spherical, but the asymmetry of the wurtzite lattice structure causes a slight elongation along the *c*-axis that is observed as a prolate deviation from a perfect spherical shape. This has been exploited in the recent preparations of CdSe nanorods (NRs) that enhance the elongation along the asymmetric axis.[16−18] Very small CdS and CdSe NPs, composed of fewer than 100 atoms, exhibit an even stronger deviation from spherical symmetry, and form, for example, tetrahedral particle shapes.[13−16] Also, since smaller NPs tend to form tetrahedral shapes, there are only certain Cd_xSe_y combinations that provide tetrahedral shapes, and these conformations would be expected to be much more stable than structures slightly larger or smaller. This notion is derived from the extensive work in metal clusters where certain "magic number" structures with enhanced stability are well-known.[19] This can be observed in experimental semiconductor NP reports, such as that by Murray et al.,[9] where a CdSe NP sample is reported to have an observed absorption onset at 414 nm.

It is known that the crystal structure of NPs can be affected by pressure, temperature, and high-intensity light.[20−23] Alivisatos discussed phase stability in NP's and related the phase preference to the ionicity of the bonding between the atoms in the lattice.[10] Chen et al. reported[20] that smaller NPs are more susceptible to structure changes induced by external forces. In the same work it was reported that the pressure-induced transformation between wurtzite and rock salt structures in CdSe was related to NP size and surface. They found that for very small NP's of 1.5 nm in diameter (effectively all surface and no volume) the pressure-induced transformation to rock salt form was highly dependent on surface interactions. Thus, solvent and capping interactions are important determinants for phase stability in small NPs.

Previous work has suggested[24] that when butylamine is added to colloidal CdSe NP's of ∼3 nm in diameter, the amine binds to the NP surface by serving as a hole trap, thereby removing these sites from participation in radiative electron−hole recombination on the surface. In this way, butylamine quenches the

† Part of the special issue "G. Wilse Robinson Festschrift".

* To whom correspondence should be addressed: mostafa.elsayed@chemistry.gatech.edu.

10.1021/jp0201130 CCC: $22.00
Published on Web 06/11/2002

fluorescence, without changing its lifetime. A similar study performed on smaller ~1 nm NPs illustrated that the role of the irregular NP surface plays an important role in the carrier recombination pathway.[25] Because of the alternate relaxation pathways in smaller NPs introduced by the multitude of surface traps, eletron-transfer induced fluorescence quenching was observed in the smaller NPs. The fluorescence of CdSe NPs in the presence of butylamine was used[25] successfully in these cases to monitor the effects of the NP surface as the NP size is decreased toward the molecular limit.

Because for very small CdSe NPs most of the Cd and Se atoms are exposed to the medium, one might expect that chemically altering the medium may introduce electronic and atomic structural changes within the NP itself that are not observed in larger NPs. In a recent communication, we reported[26] that when butylamine is added in higher concentrations (0.05−0.25 M) to small CdSe NPs, a transformation is induced either toward a "magic number" conformation and/or a phase change that absorbs at 414 nm. This transformation is observed as a decay in the original NP absorption and a corresponding growth of a new, narrower absorption feature at 414 nm that is blue-shifted with respect to the original absorption. This effect is only noted in samples of very small NPs with an absorption band-edge less than ~500 nm. Larger NPs, with an absorption onset greater than 500 nm do not exhibit this effect in the presence of butylamine within the time scale of the experiment. The current work involves the thermodynamic and kinetic study of the observed interaction between small CdSe NPs and butylamine. A possible mechanism for this interaction is discussed.

Experimental Section

Trioctylphosphine oxide (TOPO) and trioctylphosphine (TOP) capped CdSe NP's were prepared from $(CH_3)_2Cd$ (97%, Strem) and Se precursors by the method developed by Murray et al.[9] with the following modifications. After the TOPO was dried at 200 °C for 20 min, the temperature was lowered to 120 °C for NP preparation. The heating mantle was removed from the reaction vessel for injection of the precursors. After injection, the heating mantle was reapplied, and the temperature was raised very slowly to ~130−140 °C to establish a very slow and controlled growth rate. The temperature was increased over the course of ~1 h, and after each ~5 °C temperature increase, the solution was held at this temperature for 15 min to allow even growth. After the preparation was complete and the NP samples were collected, the samples were stored in the dark under argon to slow the surface degradation and Ostwald ripening processes that have been reported previously. By this method, very small NP's that are slightly over a nanometer in diameter are prepared. CdSe NP's in this size range are characterized by band-edge absorption of 400−450 nm.

Stock solutions of CdSe NP's were prepared in toluene (Aldrich). *N*-Butylamine, was used as purchased from Aldrich. Steady-state absorption spectra were performed using a Shimadzu UV-3101PC UV−vis−NIR scanning spectrophotometer. After the butylamine was placed in the NP solution, the sample was vigorously mixed for several seconds, after which the UV−vis absorption spectrum was immediately obtained. Decay curves for the absorption spectra were obtained on the same apparatus. The NP sample cuvette was placed inside the spectrophotometer. The collection was begun, after which the butylamine aliquot was added to the sample with a pipet. The pipet was used to quickly withdraw the NP/butylamine sample and reinject it to quickly stir the mixture. The injection/stirring process occurred over the course of 2−4 s and caused a spike in the absorption spectrum that immediately disappeared after stirring. This spike of 5−10 data points was removed from each data set so that an effective fit could be obtained.

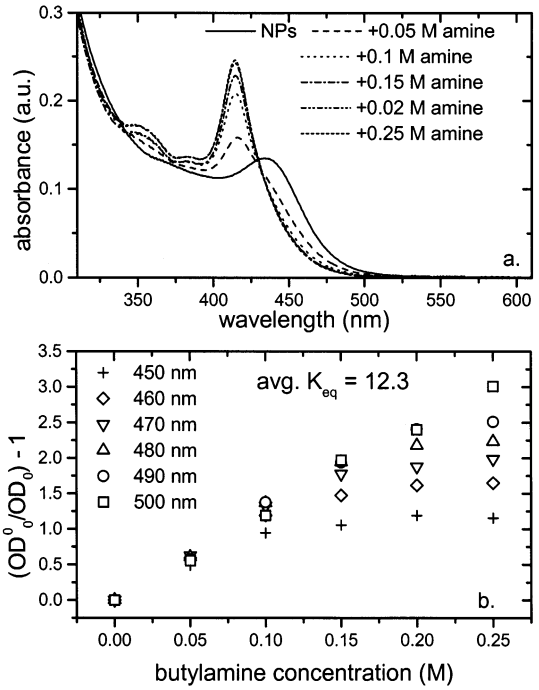

Figure 1. (a) Absorption from the original NP sample (solid curve) and absorption of the same sample after increasing amounts of butylamine have been added (other curves). The ratio of the concentration of new NPs vs that of the remaining original NPs can yield the K_{eq} for the transformation. (b) Plot of the relative concentration of the two NP species, denoted as $(OD_0^0/OD_0 - 1)$, with respect to the butylamine concentration for several wavelengths along the inhomogeneously broadened band edge. The transformation is saturated at high amine concentrations when observed at smaller wavelengths (i.e., for smaller NPs). The average slope of the best-fit line represents the K_{eq} for the interaction, 12.3.

Temperature controlled experiments were performed using a water/glycerin heat bath controlled by a TRE 100 thermostat (Neslab Instruments, Inc.). The constant temperature solution was flowed through a metal cuvette holder (machined in house) placed inside the Shimadzu spectrophotometer, in which each CdSe NP sample was placed for 15 min to equilibrate the solution temperature. A thermocouple was placed inside the metal holder to monitor the temperature throughout the experiment. Butylamine was added to the sample, the solution was stirred, and measurements were taken after 20 min to ensure that the mixture had reached equilibrium at each temperature.

A. Thermodynamic Studies. When butylamine is added to small CdSe NPs (1−2 nm), the original absorption onset decreases, and a stronger, narrower absorption feature grows at 414 nm. Figure 1a illustrates such a conversion in one NP sample. From the observed changes in the absorption spectrum, the NP sample was found to require approximately 15−20 min to reach equilibrium after the addition of butylamine. Our experiments showed us that as long as the NPs are below ~2 nm in diameter, i.e., exhibiting an absorption onset at shorter wavelengths than ~500 nm, the transformation occurs. This transformation is not observed in larger NP samples, such as the 3.2 nm NPs studied earlier by our group.[24]

The presence of the clear isobestic point shown in Figure 1a suggests that there are two interconverting species, the original NPs (NP_0) and a new NP species that is presumably a NP−

amine complex, (NP_c). This most likely results from the adsorption of butylamine to the original NPs. That the addition of increasing amounts of amine causes the transformation to occur to a greater extent suggests that we shift the equilibrium more as we add more reactants. It is interesting to notice that the new species of NPs, NP_c, with adsorbed butylamine has a narrower absorption line width than the original sample, NP_0, indicating that the interaction has somehow sharpened the size distribution.

Let us now determine the equilibrium constant for the reaction

$$NP_0 + BA \rightleftharpoons NP_c \; K_{eq} \tag{1}$$

where NP_0 is the original NP sample absorbing at 445 nm and NP_c is the new NP−amine complex absorbing at 414 nm. The equilibrium constant is given by

$$K_{eq} = \frac{[NP_c]}{[NP_0][BA]} \tag{2}$$

where [BA] is the concentration of unbound "free" butylamine. Because there is a clear isobestic point (see Figure 1a), one can safely assume that what reacts of the original NPs makes NP_c. At any concentration of butylamine, $[NP_c] = [NP_0{}^0] - [NP_0]$, where $[NP_0{}^0]$ is the initial concentration of the NPs prior to the addition of the amine. Thus,

$$K_{eq} = \frac{[NP_0{}^0] - [NP_0]}{[NP_0][BA]} \tag{3}$$

Thus by determining $[NP_0]$ once the equilibrium is reached after each addition of butylamine, one can establish $[NP_c]$ and K_{eq} can be calculated if [BA] is known. In these experiments, the NP concentration is approximately 10^{-5} M, and the butylamine concentration is ~0.1 M. At such relatively large butylamine concentrations, we do not detect any changes in the total butylamine absorption, and thus the concentration, after equilibrium has been reached. Therefore, for determining K_{eq}, we assume that [BA] is the originally added concentration.

The resulting spectrum, after equilibrium has been reached, is a combination of the spectrum of the unreacted original NPs and that of the new NPs. Since the absorption feature of the new sample is centered at 414 nm, the absorbance between 450 and 500 nm is due primarily to the unreacted NPs from the original sample. Thus, we can use the absorption in this region of the spectrum to determine $[NP_0{}^0]$ and $[NP_0]$.

Optical spectroscopy was used to determine $[NP_0]$ in the absence and after the addition of butylamine, from Beer's Law:

$$[NP_0] = \frac{OD_{NP_0}}{\epsilon_{NP_0} \ell} \tag{4}$$

where ℓ is the cell path length (1 cm), and ϵ_{NP_0} is the extinction coefficient of NP_0 at a certain wavelength. ϵ_{NP_0} was determined to be 33 300 M^{-1} cm^{-1} by the method described by Jacobsohn and Banin.[27] Briefly, a colloidal sample of known volume and optical density was dried, and the resulting solid was washed and weighed. Using the mass and average radius of the NPs, and approximating the TOPO coverage per particle, one can determine the molar extinction coefficient. Because the mass of a small NP is dominated by TOPO capping material, the approximation of TOPO coverage per NP is a substantial source of error in the calculation. The average 33 000 M^{-1} cm^{-1} value was reproducible ±5000 M^{-1} cm^{-1} and is comparable to the values presented for small CdSe clusters in ref 14. By substituting eq 4 into eq 3, K_{eq} becomes

$$K_{eq} = \frac{(OD_{NP_0{}^0} - OD_{NP_0})}{OD_{NP_0}[BA]} = \left(\frac{OD_{NP_0{}^0}}{OD_{NP_0}} - 1\right)\frac{1}{[BA]} \tag{5}$$

This equation can be rearranged to

$$\left(\frac{OD_0{}^0}{OD_0} - 1\right) = K_{eq}[BA] \tag{6}$$

A plot of $(OD_0{}^0/OD_0 - 1)$ vs [BA] should yield a straight line the slope of which is K_{eq}.

Figure 1a shows the changes in the absorption spectrum as a result of the interaction between NPs and increasing amounts of butylamine at room temperature (28 °C). Because it was observed that the transformation does not occur in samples larger than ~2 nm, it was assumed to be highly size dependent in smaller NPs. The OD_0 was monitored at several different wavelengths along the inhomogeneously broadened band edge to determine the size dependence within the sample. Figure 1b shows a plot of the relationship in eq 6, monitored at different wavelengths, which corresponds to monitoring the reaction of NPs of slightly different sizes. The experimental results yield two conclusions that can be drawn from this plot. First, at room temperature, the transformation occurs to relatively the same extent for each wavelength monitored at lower amine concentrations. Next, the transformation is saturated for shorter wavelengths (smaller sizes) at high amine concentrations. The slope of the best-fit line for each set of data, excluding the saturated values, yields a K_{eq} according to eq 6. From the slopes, the average value of K_{eq} over all wavelengths monitored is determined to be 12.3 at room temperature (25 °C).

The above experiment was repeated at different temperatures ranging from 20 to 60 °C. At temperatures much higher than 60 °C, the NPs start to grow and/or aggregate and temperatures much lower than 20 °C were not possible with the experimental apparatus. Regardless, in just this small temperature range, there was a large temperature dependence on the amount of NP_c formed. The temperature dependence for one butylamine concentration (0.25 M) is shown in Figure 2a. The inverse temperature dependence of the transformation is clear, indicating that the reaction is exothermic, i.e., its enthalpy change (ΔH_r^0) is negative. To determine the value of ΔH_r^0, we used the Van't Hoff equation:

$$\ln K_{eq} = -\frac{\Delta H_r^0}{RT} + \frac{\Delta S_r^0}{R} \tag{7}$$

Using eq 6, the K_{eq} at each temperature was calculated. Again, the values were collected at different wavelengths to examine the size dependence of ΔH_r^0 within the sample distribution. The inset of Figure 2a shows a plot of $\ln K_{eq}$ vs T^{-1}, according to eq 7, for several different wavelengths along the band-edge. The slopes of the best fit lines for the interaction were used to calculate ΔH_r^0 in each case. The size dependence of the transformation enthalpy is clear, with larger NPs having larger values of ΔH. The relationship between ΔH and band-edge absorption wavelength is shown in Figure 2b. The relationship is roughly linear within this narrow size range, and the line is included for emphasizing this relationship. The ΔH values range from 68 kJ/mol for NPs with the band edge at 500 nm to 16 kJ/mol for those with absorption onset at 450 nm. The

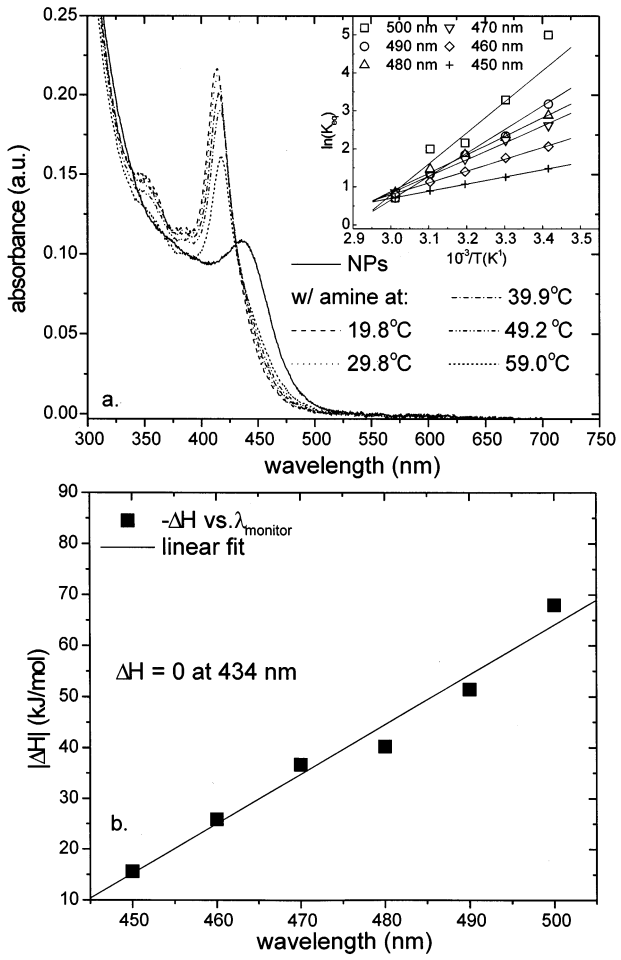

Figure 2. (a) Original NP_0 spectrum (solid curve). The additional curves show the spectrum of the NP_0 solution after 0.25 M butylamine has been added, and equilibrium has been established, at different temperatures. From the spectra, the equilibrium constant, K_{eq}, is determined at different temperatures (see text). The transformation from the original spectrum to the resulting spectrum occurs with the most intensity at the lowest temperature, 19.8 °C. The inset shows a plot of $\ln(K_{eq})$ vs T^{-1}, according to eq 7, monitored at different wavelengths along the inhomogeneously broadened band edge. The slope of each best-fit line corresponds to the ΔH of the transformation. It is clear from these data that larger CdSe NPs yield larger heats of reaction. (b) Plot of $|\Delta H|$ vs the monitoring wavelength illustrating the size dependence of the heat of transformation. The line is included to emphasize the linear relationship observed over this size range, rather than to suggest adherence to a physical model.

y-intercept of the linear fit shown in Figure 2b yields a value of 434 nm, corresponding exactly to the isobestic point that is observed in the spectra in Figure 2a.

B. Kinetic Studies. The thermodynamic data in this study were collected after the samples were allowed ∼20 min to achieve equilibrium. To monitor the time dependence of the transformation, the absorption changes were collected at single wavelengths over a period of 1000 s. The decay of the absorbance of the original NP sample was monitored at 450 nm, with several different concentrations of amine. These decay curves are shown in Figure 3. It is important to note that because we are monitoring the decay at a single wavelength, we are monitoring the decay of a narrow range of NP sizes within the inhomogeneously broadened sample. The decays were found to be biexponential in each case. There are two possible explanations for this biexponential behavior. First, it is possible that, although we monitor at a single wavelength, we are observing the changes in a distribution of NPs sizes that overlap

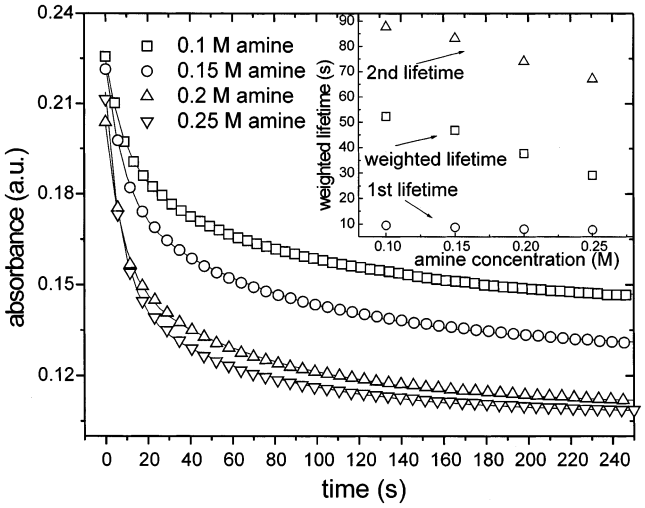

Figure 3. Time evolution of the butylamine/NP interaction at 450 nm followed as a function of amine concentration. In each case, the decay was biexponential, with lifetimes of ∼8 and ∼60−90 s for each component. The fast lifetime component of ∼8 s did not change with respect to the amine concentration. Instead, as the amine concentration increases, the relative contribution of the fast component grows. The inset shows a comparison of the changes in overall weighted mean lifetime, which accounts for the relative contribution of each component, the long component, which changes as a function of butylamine concentration, and the short component, which does not change.

TABLE 1: Lifetime Values for the Decay of the 450 nm Absorption at Different Butylamine Concentrations Seen in Figure 3

amine concn (M)	τ_1 (%)	τ_2 (%)	τ_m
0.05	9.5 s (45%)	87.6 s (55%)	52.3 s
0.10	8.7 s (49%)	83.1 s (51%)	46.9 s
0.15	8 s (55%)	73.9 s (45%)	37.7 s
0.20	7.7 s (64%)	67.1 s (36%)	29.1 s

the monitoring wavelength. This distribution of NP sizes responds in corresponding multiexponential decay in the presence of butylamine, but a biexponential fit is capable of modeling this behavior.

Also, it is possible that the biexponential behavior of the decays shown in Figure 3 suggests that the interaction between the amine and the original NP solution may not be as straightforward as eq 1 indicates. A true biexponential decay would indicate that the reaction is not first order and that there is some mesostable intermediate state through which the transformation must pass before the NPs reach equilibrium. The biexponential fit in each case yields unchanging values for the first lifetime component, approximately 8 s. At higher amine concentrations, however, the relative amplitude of the short component increases. At the same time, the lifetime of the second component decreases. This causes the weighted mean lifetime, τ_m, of the decay, given by

$$\tau_m = \frac{a_1\tau_1 + a_2\tau_2}{a_1 + a_2} \tag{8}$$

to change dramatically as a function of amine concentration. In eq 8, the preexponential factor of each lifetime component is a_i, and τ_i represents each lifetime. A comparison of the first, second, and weighted mean lifetime at each amine concentration is shown graphically in the inset of Figure 3. The individual values for the first and second lifetime components, as well as the weighted mean lifetime, are shown in Table 1.

The unchanging value of the short lifetime in comparison to the dramatically changing values of the second lifetime and the

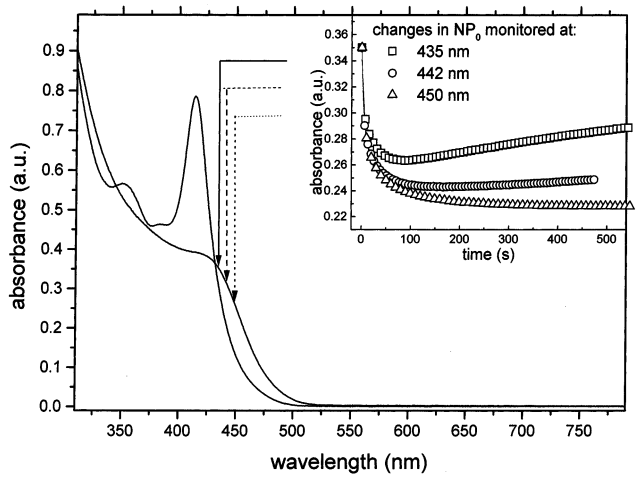

Figure 4. Decay of the original NP spectrum followed at several wavelengths along the inhomogeneously broadened band edge. The inset shows the decay curves measured at 435 nm (near the isobestic point), 442 nm, and 450 nm, corresponding to the transformation of successively larger NPs. The decay curves show that the transformation occurs more slowly for NPs of larger sizes.

TABLE 2: Lifetime Values for Decays in Original NP Absorbance Monitored at Different Wavelengths[a]

wavelength monitored (nm)	τ_1 (%)	τ_2 (%)	τ_m
435	2 s (63%)	19 s (37%)	8 s
442	3 s (53%)	29 s (47%)	15 s
450	7 s (63%)	70 s (37%)	30 s

[a] The data are presented graphically in Figure 4.

overall contribution of each indicate that there are two distinct processes occurring after the butylamine has been added. The experimental data suggest that the first-order optical transformation that we observe is actually a result of the combination of these two underlying processes.

Because the transition enthalpy is highly dependent on the original NP size, it is interesting to examine the decay kinetics at different NP sizes as well. Figure 4 illustrates the results of such an experiment. The decay values were followed at 435, 442, and 450 nm through 1000 s. Decays for longer wavelengths are not included because the overall signal is smaller at these values and the transformations required a longer time period. The trend, however, is the same over the inhomogeneously broadened band edge. The first lifetime value comprises ~60% of the overall decay kinetics and remains at ~4 s. The second lifetime value, in comparison, changes dramatically from 19 s at 435 nm to 70 s at 450 nm. The lifetime values are included in Table 2.

There are two interesting points to observe in the decays at different wavelengths shown in Figure 4. The decay of the original feature is necessary for the transformation in the presence of butylamine to occur. This decay occurs more slowly for larger NPs, indicating that larger NPs experience a higher kinetic barrier to transformation than smaller NPs. Also, we can observe in Figure 4, at the isobestic point of 435 nm, the decay of the original feature that occurs very quickly, within 20 s, followed by the slow rise resulting from homogeneously broadened growth of the 414 nm feature.

Because of the obvious kinetic barrier that exists in the transformation, it is necessary to derive the activation energy for the transformation at a single wavelength. That the decays appear to be truly biexponential suggests that using a weighted mean lifetime in an Arrhenius plot will only give an averaged

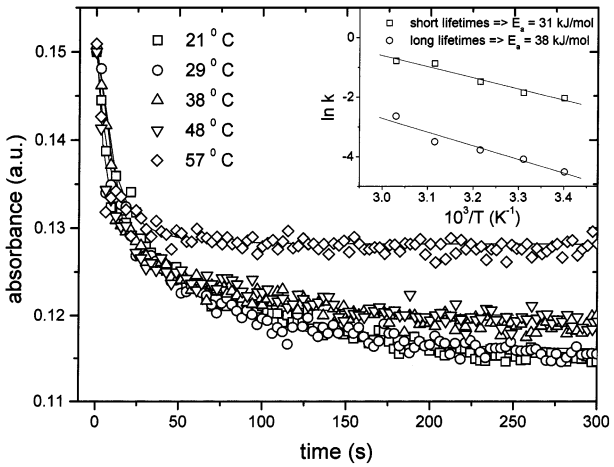

Figure 5. Time evolution of the interaction between butylamine and CdSe NPs monitored at different temperatures. The decay of the absorbance of the NPs at 450 nm is followed immediately after the addition of butylamine. In each case, the decay of the original spectrum is biexponential. The decay process occurs more quickly at higher temperatures, but to a lower extent because the process is exothermic. (Inset) the changes in each lifetime with respect to temperature are used to calculate the activation energy for each process. A plot of ln k vs T^{-1} was shown to be linear in each case. The slope of each best-fit line was used to calculate E_a for the slow and fast processes, 31 and 38 kJ/mol, respectively.

TABLE 3: Lifetime Values from Arrhenius Data Shown in Figure 5 for the Decrease in the 450 nm Absorption Feature after Butylamine Is Added to the NP Solution[a]

temp (K)	τ_1 (%)	τ_2 (%)	τ_m
292.8	7.7 s (46%)	91.1 s (54%)	52.5 s
302.8	6.4 s (48%)	59.6 s (52%)	30.9 s
312.9	4.4 s (54%)	43.6 s (46%)	22.6 s
322.2	2.4 s (45%)	33.2 s (54%)	19 s
332	2.2 s (50%)	14 s (50%)	8.2 s

[a] τ_1 is the short lifetime, τ_2 is the long lifetime, and τ_m is the weighted mean lifetime, according to eq 8.

overall value for the activation energy of the total process. It is more appropriate to calculate the activation energy for each physical process. The decay of the absorbance of the original NP sample after the amine was added was studied in the temperature range between 20 and 60 °C. The results are shown in Figure 5. A plot of ln k vs T^{-1} is shown for both the short and long lifetimes in the inset of Figure 5 according to the Arrhenius equation. The linear fit of this relationship was used to calculate the overall activation energy of the transformation of the original NP sample and found to be 31 kJ/mol for the first component and 38 kJ/mol for the second component. Table 3 shows the values for the individual lifetimes at each temperature, as well as the weighted mean lifetime, according to eq 8.

The data from the decays of the original absorption feature at different amine concentrations, temperatures, and wavelength, as well as the thermodynamic experiments, have suggested that the transformation process occurs to a different extent and at different rates for NPs of different original size. Thus, the rise in the 414 nm absorption feature may be expected to have complicated thermodynamic and kinetic behavior. Because its absorption lies within the higher order band structure of the original NP absorption, the resulting absorption intensity that we observe occurs from a combination of the disappearance of the original spectrum and the appearance of the new feature. The decay/rise trace of the 435 nm absorption feature shown in Figure 4 illustrates this behavior. Also, because the original NP distribution is transformed to the new NPs at different rates

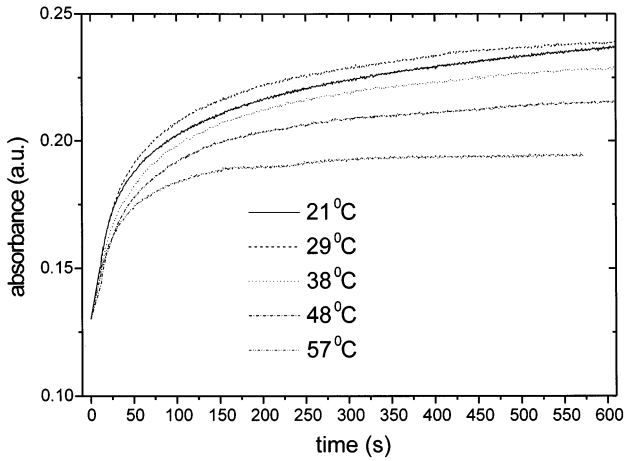

Figure 6. Nonexponential dynamics of the rise in the 414 nm absorption feature. In comparison to the decays shown in Figure 6, which are complete within 300−400 s, the 414 nm peak has a much longer rise time, presumably because it exhibits contributions from the inhomogeneously broadened original NP sizes.

depending on their size, the 414 nm absorption should be expected to rise at a rate corresponding to a convolution of the rates of disappearance of the ensemble of original NPs. Figure 6 illustrates the rise kinetics of the 414 nm peak measured at temperatures similar to those used in the decay experiments. These data exhibit the same temperature dependence as the thermodynamic/decay data. The transformation occurs to a greater extent at lower temperatures but occurs more quickly at higher temperatures. However, the rise kinetics in all cases are completely nonexponential, as expected given the contribution from transformations of different NP sizes at different rates.

Discussion

Many studies have described the size and shape transformations in NPs induced by different perturbations. The Alivisatos group has focused on phase transformations between wurtzite and rock salt forms induced by pressure.[23] Yakovlev et al. have reported[22] the size and shape transformation of CdS NP's using second harmonic light from a pulsed Nd:YAG laser. Additionally, S. B. Qadri et al.[28] studied the temperature dependence phase transition of ZnS NPs from zinc blend to wurtzite using powder X-ray diffraction. Zinc blend is the thermodynamically stable form of bulk ZnS, but it can be transformed to the wurtzite form at high temperatures. The group noted that the transition for bulk ZnS occurs at 1020 °C but observed that the transformation occurred between 300 and 500 °C in 2.8 nm NPs. They were unable to obtain exact thermodynamic values for the decrease in transition temperature because equilibrium was not established. These experiments reveal, however, that there is a decrease in the energy required to transform NPs from one phase to another relative to the bulk values. These results are supported by Banerjee et al.[29] who report that for CdS NPs there is a critical particle size above which the hexagonal wurtzite phase is stable and below which the cubic zinc blend structure predominates. The authors also suggest that this size-dependent phase transition between wurtzite and zinc blend also contributes to the observed optical properties because the two phases have slightly different band-gap values.

The current experiment, like those reported in the literature, emphasizes the relationship between NP size, surface, structure, and optical properties. The transformation that we observe in CdSe NPs in the presence of butylamine requires that the NP size be very small. As the NP size is decreased, several factors contribute to the physical and chemical stability of the particles. For instance, the curvature of the NP surface increases as the size decreases. The increased curvature leads to an increased surface free energy. Thus the increase in the free energy in small NPs leads to a decrease in their melting temperature, as described by Valov and Leiman[30] in their study of CuCl NPs. A surface free energy that is high compared with the stabilizing effects of capping material is one feature of small NPs. For example, compared to NPs larger than 2 nm in diameter, small NPs require an excess of capping material in solution to keep them suspended in the solvent. The centrifugation process that removes excess capping material from larger NP samples causes smaller NPs to fall out of solution. Without an excess of capping material, the NPs will not suspend in common organic solvents. Also, the interaction with oxygen and light that causes the surface of larger NPs stored in the laboratory to gradually degrade over the course of several weeks occurs in days with smaller NPs. This requires that small NP samples be carefully stored under argon in the dark in order that they do not aggregate and/or degrade. These observations confirm that the surface of very small NPs is unstable with respect to the binding of the TOPO capping material and the interaction with impurities such as oxygen.

These empirical observations, along with the experimental conclusion that butylamine can effectively bind to the NP surface,[24,25] lead us to suggest that the initial process in the butylamine/small NP interaction is the substitution of butylamine for the TOPO capping material, as has been observed with pyridine. Because the butylamine concentration required to induce the change in the spectrum is high with respect to the NP concentration, the reaction is not diffusion limited and becomes pseudo-first-order with respect to the NPs but not with respect to the butylamine concentration. Thus, the kinetics of this process would not be affected by increasing the amount of butylamine in the solution. Increasing the amount of butylamine would only increase the amount of butylamine that binds to the surface.

The binding process releases energy, which, combined with the already low surface stability of the small NP, allows the NP to break and re-form Cd−Se bonds. This slower process would be the rate determining step in the transformation. Because it relies upon the energy released by the binding of butylamine with the NP surface, this process would be dependent on the amount of butylamine present. As more butylamine molecules displace TOPO and bind with the NP surface, more energy is released by the interaction. Consequently, the rearrangement to the more thermodynamically stable NP sample occurs more quickly. This reaction-driven rearrangement allows these small CdSe NPs, in the presence of butylamine, to reestablish a new equilibrium size and/or structure that is more stable than the previous form. The NP size-dependent transformation can also be observed in the multiexponential rise in the 414 nm feature that results from the conversion of an ensemble of original NP sizes at their respective size-dependent rates.

It has been observed that CdSe with a magic number structure absorbs at 414 nm.[9] Theoretical predictions have found that some CdSe clusters are more stable in the zinc blend lattice than in the wurtzite form.[15] In light of these studies and the present results, we suggest that the observed transition is either chemically induced etching to a more stable size having a magic number of Cd_xSe_y, a reorganization to a more stable lattice, or some combination of these two changes. Any calculation of a theoretical transition energy for this transformation with the

presence of amine requires the consideration of the structural and electronic energies of both the wurtzite and zinc blend CdSe, bond energies of Cd−Se both within the NP and on the surface, Cd and Se capping material bond energies, and ionic/covalent radii for all the atoms involved. The different possible reactions that can take place and give rise to the observed exothermicity due to the formation of the amine complex are

$$n\mathrm{A} + \mathrm{NP}_0{}^0 \rightarrow \mathrm{NP}_c \tag{9}$$

$$n\mathrm{A} + \mathrm{NP}_0{}^0 \rightarrow \mathrm{NP}_c + n\mathrm{T} \tag{10}$$

$$n\mathrm{A} + \mathrm{NP}_0{}^0 \rightarrow \mathrm{NP}_c + m\mathrm{CdSe} \tag{11}$$

$$n\mathrm{A} + \mathrm{NP}_0{}^0 \rightarrow \mathrm{NP}_c + m\mathrm{CdS} + n\mathrm{T} \tag{12}$$

where A, $NP_0{}^0$, NP_c, T, and CdSe represent respectively the amine, the original NPs, the amine−particle complex, TOPO, and CdSe molecules that are desorbed from the NP to create the magic number structure. The amine displaces the TOPO capping material in reactions 10 and 12. In reactions 9 and 11, the amine adsorbs on empty surface sites. A number of CdSe molecules are released to yield a magic number CdSe NP structure in reactions 11 and 12. In addition, for each reaction above, NP_c could be in a different crystalline phase from that of $NP_0{}^0$. It is clear from the above that it is difficult to calculate the ΔH_r for the observed transformation. Even for one of the above reactions (eq 9), it is difficult as shown below to calculate ΔH_r.

$$\Delta H_r = \Delta H_f(\mathrm{NP}_c) - n\Delta \mathrm{H}_f(\mathrm{A}) - \Delta H_f(\mathrm{NP}_0{}^0) \tag{13}$$

where $\Delta H_f(A)$ might be calculated from its gas-phase value and its solvation energy. However, the calculation of $\Delta H_f(NP_c)$ with the amine adsorbed on the NP surface, which can be in one phase or another is beyond the scope of this experimental study. Alternatively, one might discuss the origin of the observed exothermicity qualitatively.

The exothermicity of the reaction is due to formation of the amine−NP bond (eq 9) and the stability of the new size/phase of the resulting nanocrystal. In eq 10, the amine−NP bonds must be stronger than the TOPO−NP bonds or else the difference is smaller than the energy of the phase changes. The attainment of a magic number, the solvation energy of the released CdSe ions, as well as the amine−NP bonds, must contribute to the observed exothermicity in eq 11. In eq 12, the difference between the amine−NP and the TOPO−NP bond energies might be a contributor to the observed exothermicity.

Conclusion

In conclusion, we have observed an exothermic transformation of small CdSe NPs in the presence of butylamine. This transformation yields a more monodisperse NP sample that absorbs with a higher band gap energy than the original solution. The implications of this transformation are that the butylamine induces a size optimization, a phase transformation, or some combination of the two processes.

Acknowledgment. This research was funded by ONR grant no. N00014-95-1-0306. We thank the reviewers for helpful comments. C.L. thanks Dr. M. Braun for helpful discussions that led to a more complete analysis of the thermodynamic data. Also, C.L. thanks the Office of Naval Research for partial support through a Molecular Design Institute fellowship.

References and Notes

(1) Bowker, M.; Bennett, R. A.; Dickinson, A.; James, D.; Smith, R. D.; Stone, P. *Stud. Surf. Sci. Catal.* **2001**, *133*, 3.
(2) O'Regan, B.; Graetzel, M. *Nature* **1991**, *353*, 737.
(3) Klimov, V. I.; Mikhailovsky, A. A.; Xu, Su; Malko, A.; Hollingsworth, J. A.; Leatherdale, C. A.; Eisler, H.-J.; Bawendi, M. G. *Science* **2000**, *290*, 314.
(4) Nayfeh, M. H.; Barry, N.; Therrien, J.; Akcakir, O.; Gratton, E.; Belomoin, G. *Appl. Phys. Lett.* **2001**, *78*, 1131.
(5) Spanhel, L.; Haase, M.; Weller, H.; Henglein, A. *J. Am. Chem. Soc.* **1987**, *109*, 5649.
(6) Hines, M. A.; Guyot-Sionnest, P. *J. Phys. Chem.* **1996**, *100*, 468.
(7) Dabbousi, B. O.; Rodriguez-Viejo, J.; Mikulec, F. V.; Heine, J. R.; Mattoussi, H.; Ober, R.; Jensen, K. F.; Bawendi, M. G. *J. Phys. Chem. B* **1997**, *101*, 9463.
(8) Talapin, D. V.; Haubold, S.; Rogach, A. L.; Kornowski, A.; Haase, M.; Weller, H. *J. Phys. Chem. B* **2001**, *105*, 2260.
(9) Murray, C. B.; Norris, D. J.; Bawendi, M. G. *J. Am. Chem. Soc.* **1993**, *115*, 8706.
(10) Alivisatos, A. P. *J. Phys. Chem.* **1996**, *100*, 13226.
(11) Lifshitz, E.; Dag, I.; Litvitn, I. D.; Hodes, G. *J. Phys. Chem. B* **1998**, *102*, 9245.
(12) Herron, N.; Clabrese, J. C.; Farneth, W. E.; Wang, Y. *Science* **1993**, *259*, 1426.
(13) Vossmeyer, T.; Rech, G.; Schulz, B.; Katsikas, L.; Weller, H. *J. Am. Chem. Soc.* **1995**, *117*, 12881.
(14) Soloviev, V. N.; Eichhofer, D.; Fenske, D.; Banin, U. *J. Am. Chem. Soc.* **2000**, *122*, 2673.
(15) Eichkorn, K.; Ahlrichs, R. *Chem. Phys. Lett.* **1998**, *288*, 235.
(16) Peng, Xiaogang; Manna, L.; Weidong, Y.; Wickham, J.; Scher, E.; Kadavanich, A.; Alivisatos, A. P. *Nature* **2000**, *407*, 981.
(17) Manna, L.; Scher, E. C.; Alivisatos, A. P. *J. Am. Chem. Soc.* **2000**, *122*, 12700.
(18) Peng, Z. Adam; Peng, Xiaogang *J. Am. Chem. Soc.* **2001**, *123*, 1389.
(19) Castleman, A. W.; Bowen, K. H. *J. Phys. Chem.* **1996**, *100*, 12911.
(20) Chen, C. C.; Herhold, A. B.; Johnson, C. S.; Alivisatos, A. P. *Science* **1997**, *276*, 398.
(21) Wickham, J. N.; Herhold, A. B.; Alivisatos, A. P. *Phys. Rev. Lett.* **2000**, *84*, 923.
(22) Yakovlev, V. V.; Lazarov, V.; Reynolds, J.; Gajdardziska-Josifovska, M. *Appl. Phys. Lett.* **2000**, *76*, 2050.
(23) Tolbert, S. H.; Alivisatos, A. P. *Science* **1994**, *265*, 373.
(24) Landes, C. F.; Burda, C. B.; Braun, M.; El-Sayed, M. A. *J. Phys. Chem. B* **2001**, *105*, 2981.
(25) Landes, C. F.; Braun, M.; El-Sayed, M. A. *J. Phys. Chem. B* **2001**, *105*, 10554.
(26) Landes, C. F.; Burda, C.; Braun, M.; El-Sayed, M. A. *Nano Lett.* **2001**, *1*, 667.
(27) Jacobsohn, M.; Banin, U. *J. Phys. Chem. B* **2000**, *104*, 1.
(28) Qadri, S. B.; Skelton, E. F.; Hsu, D.; Dinsmore, A. D.; Yang, J.; Gray, H. F.; Ratna, B. R. *Phys. Rev. B* **1999**, *60*, 9191.
(29) Banerjee, R.; Jayakrishnan, R.; Ayyub, P. *J. Phys.: Condens. Matter* **2000**, *12*, 10647.
(30) Valov, P. M.; Leiman, V. I. *Phys. Solid State* **1999**, *41*, 278.